

DISTRIBUTION OF TWO-PHASE FLOW IN A DISTRIBUTOR

AZRIDJAL AZIZ^{1,2}, AKIO MIYARA^{1,*}, FUMIAKI SUGINO¹

¹Department of Mechanical Engineering, Saga University,
1 Honjomachi, Saga-shi, 8408502, Japan

²Department of Mechanical Engineering, Riau University
Kampus Bina Widya, Km 12,5, Sp. Baru, Panam, Pekanbaru, 28293, Indonesia

*Corresponding Author: miyara@me.saga-u.ac.jp

Abstract

The flow configuration and distribution behavior of two-phase flow in a distributor made of acrylic resin have been investigated experimentally. In this study, air and water were used as two-phase flow working fluids. The distributor consists of one inlet and two outlets, which are set as upper and lower, respectively. The flow visualization at the distributor was made by using a high-speed camera. The flow rates of air and water flowing out from the upper and lower outlet branches were measured. Effects of inclination angle of the distributor were investigated. By changing the inclination angle from vertical to horizontal, uneven distributions were also observed. The distribution of two-phase flow through distributor tends even flow distribution on the vertical position and tends uneven distribution on inclined and horizontal positions. It is shown that even distribution could be achieved at high superficial velocities of both air and water.

Keywords: Two-phase flow, Distributor, Distribution, Visualization, Angle.

1. Introduction

Flow mal-distribution of two-phase flow mixtures in heat exchangers with parallel flow circuits reduce the thermal performance where the heat transfer occurs. Often, flow rates through the channels are not uniform and in the extreme case, almost no flow through some of them, which exhibits a poor heat exchanging performance. The situation becomes more complicated especially with two-phase flows [1]. In evaporators, uniform distribution is essential to avoid dry-out phenomenon and the resulting poor heat exchange performance. In condensers, uneven distribution of liquid could create zones of reduced heat transfer due to high liquid loading. Thus,

Nomenclatures

A	Area, m ²
Q	Volumetric flow rate, L/min
R	Deviation ratio
U	Superficial velocity, m/s

Subscripts

1	Outlet 1
2	Outlet 2
G	Gas phase, air
L	Liquid phase, water

in the design and optimization of compact heat exchangers with parallel flow technologies, understanding of two phase distribution in the manifolds are great importance [2-4].

Tae and Cho [5] have investigated two-phase flow distribution and phase separation through various types of branch tubes in single T-junction. Wen et al. [6] investigated how to improving two-phase refrigerant distribution in the manifold of the refrigeration system with three different distributor configuration. Many variables affect the distribution of two-phase mixtures, including geometric factors (manifold cross-section design, branch couplings, location, and orientation of the tubes) and on the inlet flow conditions (flow rate, flow structure, vapor fraction, and heat load on the tubes). Due to this complexity, no general physically based method has been developed to describe the flow conditions in heat exchanger manifolds and predict the two-phase flow distribution. Kim and Sin [7] studied air and water two-phase flow distribution in a parallel flow heat exchanger. Due to complexity, only a limited number of studies have investigated the phenomenon that occurs in two-phase flow distributors.

Recently, the use of small diameter tube is becoming of interest in improving the heat exchanger performance, but a large pressure drop will be occur in the small tube and it would be decrease the heat transfer performance. In order to reduce the pressure drop and to obtain a higher heat transfer coefficient of refrigerant flow, the flow must be distributed into several channels by using a distributor. The refrigerant distributor will distribute refrigerant flow equally from the thermostatic expansion valve into each evaporator channel.

To keep the heat exchanger performance, refrigerant should be distributed equally through each pipe. However, the refrigerant flow through distributor is not easy flow divided equally, and the drift condition of the refrigerant flow will be influenced by the shape and position of the distributor. Sometimes, it could be lead to decrease of heat exchanger performance. It is necessary to maintain the performance of the heat exchanger by minimizing this drift condition. In air conditioners, vapor and liquid of a refrigerant flow through distributor. Although air and water flow in the distributor is somewhat different from the two-phase refrigerant flow, experiments of the distribution of air-water two-phase flow give valuable information. Flow observations are possible only for air and water flow.

In this study, experimental research is aimed to clarify general characteristics of flow and deviation of air-water two-phase flows through the distributor. The

flow rates of each phase flowing in the outlet after distributor branches upper and lower were measured. To understand the two-phase flow behavior in the distributor, flow distribution patterns of air and water have been observed by a high-speed camera. Effects of inclination angle of the distributor on flow pattern and flow rate of air and water were also investigated.

2. Experiments

2.1. Experimental apparatus and procedure

Figure 1 illustrates the experimental apparatus. The experimental apparatus consists of air and water supply system, merging section, distributor test section, two gas-liquid separator, air measuring bath, and water measuring cylinder. Air flow rate and water flow rate before entering to test section are set up using a flow meter and air-water will mix in the merging section.

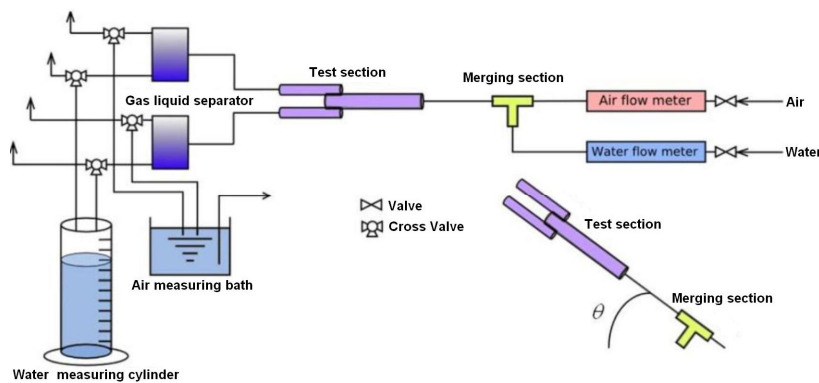


Fig. 1. Experimental Apparatus.

The test section consists of an entrance tube with diameter of 8 mm and a distributor with two outlet tubes, upper and lower with diameter of 5 mm. The entrance tube has 400 mm tube length from the distributor inlet to ensure a fully developed flow. The distributor was machined and polished from a rectangular block of acrylic resin. The transparent block facilitates flow visualization observation. To investigate the slope effect of the distributor, the angle direction of the test section can be changed to other angle. The whole test section and the detail of the distributor are shown in Figs. 2 and 3, respectively. In this study air and water were used as two-phase flow working fluid. Water was supplied by water source in laboratory. Air was supplied by air-compressor with set up pressure regulator. Both the air and water flow rate were controlled by using calibrated rotameter before entering the merging section. The accuracy of the rotameter is $\pm 6\%$.

The experiments were conducted in different slopes of the distributor in 0° , 45° and 90° with varying air and water flow rates. The inclination angle 0° is used for horizontal position, 45° for inclined position and 90° is used for vertical position. The measurements of air and water flow rates at each exit of distributor were taken after the gas-liquid separator. Air flow rate was measured by the air measuring bath and water flow rate by the water measuring cylinder. The flow

visualization and photographs of flow patterns were captured using high speed video camera (Keyence Motion Analyzing VW-6000) at shutter speed 1/30.000 second, frame rate per second (fps) at 500 fps, and reproduction speed at 15 fps. During the whole series of tests, several runs were made to check the repeatability of the data. The data presented are average values of ten measurements. The errors of the air and water flow rate measurements are considered to be acceptable and they are evaluated as 6.14% and 5.19%, respectively.

The uncertainties were estimated using the method suggested by Bell [8] and Moffat [9]. The measurement uncertainties of the air and water flow rates were $\pm 4.0\%$ and $\pm 1.9\%$, respectively.



Fig. 2. Test Section.

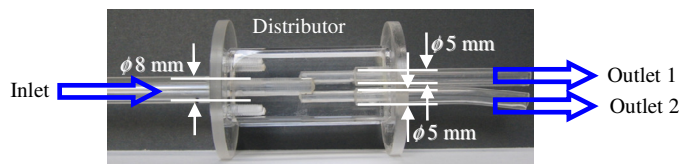


Fig. 3. Distributor.

2.2. Data reduction

The air-water volumetric flow rate was taken after flow out from the gas-liquid separator. The volumetric flow rates of air in outlet 1 and outlet 2 are Q_{G1} and Q_{G2} and the volumetric flow rates of water are Q_{L1} and Q_{L2} , respectively. The deviation ratio R defined with Eqs. (1) and (2). The air deviation ratio is R_G , and the water deviation ratio is R_L . Where, subscript G is for air and subscript L for water.

$$R_G = (Q_{G1} - Q_{G2}) / (Q_{G1} + Q_{G2}) \quad (1)$$

$$R_L = (Q_{L1} - Q_{L2}) / (Q_{L1} + Q_{L2}) \quad (2)$$

$R = 1$ states that all fluid flow out from the upper outlet, $R = 0$ states that there is no deviation, and $R = -1$ states that all fluid flow out from the lower outlet.

The superficial velocities U of each fluid are defined with Eqs. (3) and (4). U_G is the air superficial velocity and U_L is the water superficial velocity.

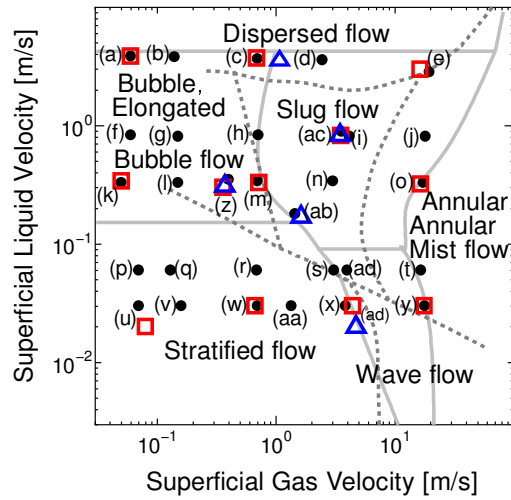
$$U_G = Q_G / A \quad (3)$$

$$U_L = Q_L / A \quad (4)$$

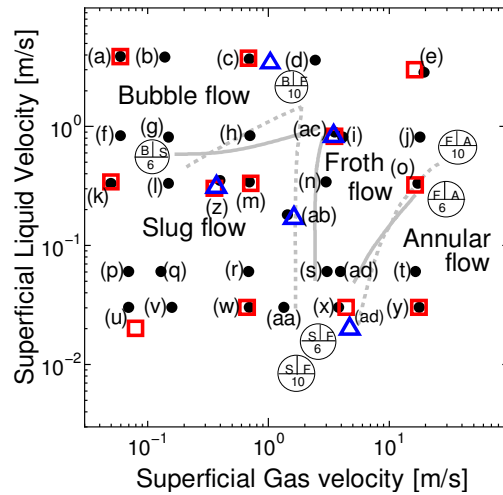
where A is flow area of inlet tube.

3. Results and Discussion

The experimental conditions are plotted on flow pattern maps as shown in Figs. 4(a) and 4(b), which are Mandhane map for horizontal flow and Sekoguchi map for vertical flow. In Fig. 4(a), solid lines indicate criteria of Mandhane et al. [10] and dashed lines indicate criteria of Baker [11]. The Sekoguchi map [12] is for upward and concurrent vertical flow. Three types of symbols mean different inclination, such as black circle for 0°, square for 45°, and triangle for 90°.



(a) Mandhane [10] and Baker [11] Maps for Horizontal Flow.



(b) Sekoguchi [12] Map for Vertical Flow.

Fig. 4. Experimental Conditions on Flow Pattern Maps.

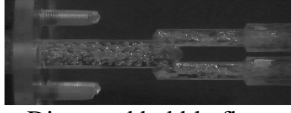
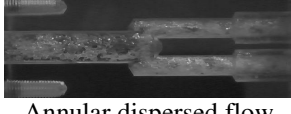
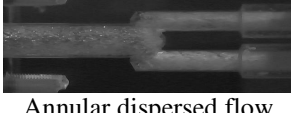
The experiment was carried out on the condition of the water superficial velocity U_L is constant with changing conditions of air superficial velocity U_G

from low to high or vice versa. Experimental data have been obtained under the conditions of superficial velocities of air and water, which are 0.06, 0.15, 0.7, 3.31, 17.92 m/s for air and 0.03, 0.06, 0.33, 0.82, 3.54 m/s for water, respectively.

In the present experiment, developed two-phase flows, which are achieved before the distributor, agree to these flow pattern maps for both the conditions of horizontal and vertical. The experiments cover stratified flow, wavy flow, elongated bubble flow, dispersed flow, slug flow, bubble flow, and annular flow. Identification of the flow patterns were carried out using flow patterns suggested by Massoud [13] and Ghiaasiaan [14]. The experiments of different distributor inclination angle at 0° , 45° and 90° were conducted under same superficial velocity condition, though they are some discrepancies.

Typical photographs of the observed flow patterns for distributor position 0° (horizontal) are shown in Table 1 that corresponding with point *a*, *b*, *c*, *d*, and *e*, where the air superficial velocity is varied from low to high (0.06 m/s to 19.57 m/s) and water superficial velocity is kept at high velocity, around 3.54 m/s.

Table 1. Observed Flow Pattern for Point of *a*, *b*, *c*, *d*, and *e* at High Superficial Velocities of Water relatively Constant and varies of Air from Low to High at Distributor Position 0° .

Flow Pattern Image	Point	Superficial Velocity	Deviation Ratio
 Dispersed bubbly flow	<i>a</i>	$U_G = 0.06$ m/s $U_L = 3.85$ m/s	$R_G = 0.198$ $R_L = -0.041$
 Dispersed bubbly flow	<i>b</i>	$U_G = 0.14$ m/s $U_L = 3.80$ m/s	$R_G = 0.036$ $R_L = -0.059$
 Dispersed bubbly flow	<i>c</i>	$U_G = 0.70$ m/s $U_L = 3.66$ m/s	$R_G = 0.255$ $R_L = -0.018$
 Annular dispersed flow	<i>d</i>	$U_G = 2.46$ m/s $U_L = 3.58$ m/s	$R_G = 0.486$ $R_L = -0.075$
 Annular dispersed flow	<i>e</i>	$U_G = 19.57$ m/s $U_L = 2.83$ m/s	$R_G = 0.091$ $R_L = -0.023$

For the all conditions, the water deviation ratios R_L are negative though they are close to zero as shown in Table 1. It showed that the evenly distribution of water on the distributor in upper outlet and lower outlet could achieved at the high water superficial velocity with increasing of the air superficial velocity.

On the other hand, the air deviation ratios R_G are positive and it is not simple variation. Increasing the air superficial velocity, R_G decreases first, increases, and decreases again. The flow pattern of these conditions is varied as follows. At the points a and b , small bubbles are uniformly distributed though the point b is more uniform. However, the flow pattern becomes the annular dispersed flow at point d where the air slug tends to flow upper part of the tube. Increasing air velocity, the flow is more disturbed and air is evenly distributed. In the high water velocity region, the water flow is dominant and the air velocity has insignificant effect.

The flow pattern identification by visual observation is quite subjective, it is necessary to define the associated flow pattern in details. The description of flow pattern on Mandhane [10] and Baker [11] flow pattern map given in Fig. 4(a) agree with the flow pattern image as shown in Table 1.

This flow pattern cover dispersed bubbly flow and annular dispersed flow for high liquid superficial velocity and it is agree with flow pattern from Massoud [13] and Ghiaasiaan [14]. It can be concluded that the equal liquid distribution, which is required to keep high performance of evaporator, is only accomplished under the condition of high vapor and liquid velocities.

The experimental results with typical photograph for point of y , t , o , j , and e at distributor position 0° (horizontal) are shown in Table 2. The air superficial velocity is kept at high velocity, around 18 m/s, and water superficial velocity is varied from 0.03 m/s to 2.83 m/s. The air deviation ratios R_G are positive for all the conditions, though they are rather close to zero as shown in Table 2.

It indicated that even if the high air superficial velocity, the air flow slightly drifts to upper outlet independently of water flow rate. On the other hand, the water deviation ratios R_L are negative though the value is approaching zero with a gradual increasing of water superficial velocity.

The visualized flow regime (see Table 2) can be further classified into annular flow, annular mist flow, and annular dispersed flow. It can be confirmed with Mandhane [10] and Baker [11] flow pattern map as shown in Fig. 4(a). It can be explained that from Table 2 the uniform distribution of air was obtained at higher air velocity, where at these condition R_G approaches zero. The more uniform distribution for water can be achieved with increasing water velocity.

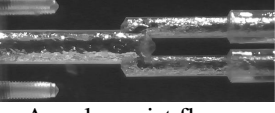
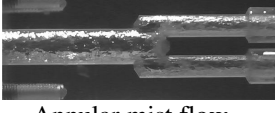
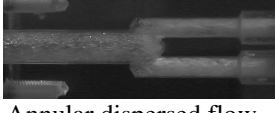
Figure 5 shows the experimental results of distributor position 0° (horizontal) with deviation ratio on superficial velocities of air and water which are 0.06, 0.15, 0.7, 3.31, 17.92 m/s for air and 0.03, 0.06, 0.33, 0.82, 3.54 m/s for water, respectively. Figure 5(b) shows the flow pattern map of Mandhane [10] and Baker [11] for horizontal position with circle mark for experimental results.

At water superficial velocity constant on 0.03, 0.06, 0.33, 0.82, 3.54 m/s with air superficial velocity is varied from low to high (0.06 m/s to 17.92 m/s) as shown in Fig. 5(a), the flow distribution of air in the distributor tends to evenly distributed at high air superficial velocity, the air deviation ratios R_G in this condition is positive though they are rather close to zero.

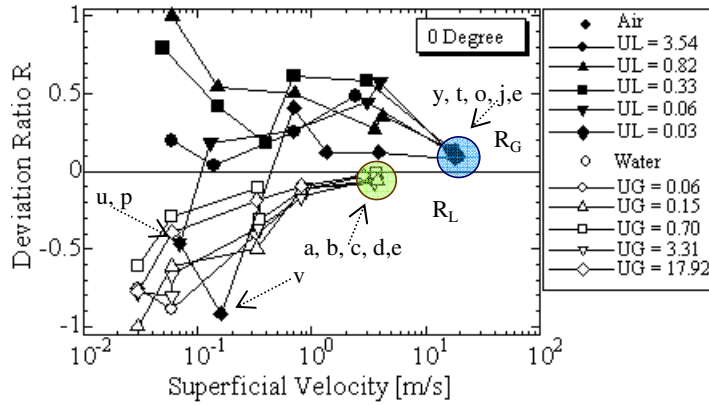
On the other hand, at air superficial velocity constant on 0.06, 0.15, 0.7, 3.31, 17.92 m/s with water superficial velocity is varied from low to high (0.03 m/s to 3.54 m/s) as shown in Fig. 5(a), the flow distribution of water in the distributor tends to evenly distributed at high water superficial velocity.

The water deviation ratios R_L in this condition is negative, though the value is approaching zero with increasing water superficial velocity. So it can be stated that the deviation ratios R are approaching zero or it tends evenly flow distribution through the distributor at high superficial velocities of air and water.

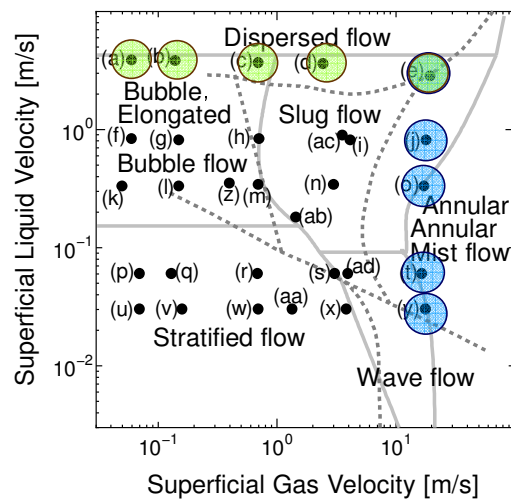
Table 2. Observed Flow Pattern for Point of $y, t, o, j,$ and e at High Superficial Velocities of Air relatively Constant and varies in Water from Low to High at Distributor Position 0° .

Flow Pattern Image	Point	Superficial Velocity	Deviation Ratio
 Annular flow	y	$U_G = 17.90$ m/s $U_L = 0.03$ m/s	$R_G = 0.082$ $R_L = -0.773$
 Annular flow	t	$U_G = 16.64$ m/s $U_L = 0.06$ m/s	$R_G = 0.114$ $R_L = -0.391$
 Annular mist flow	o	$U_G = 17.38$ m/s $U_L = 0.33$ m/s	$R_G = 0.134$ $R_L = -0.185$
 Annular mist flow	j	$U_G = 18.11$ m/s $U_L = 0.81$ m/s	$R_G = 0.133$ $R_L = -0.093$
 Annular dispersed flow	e	$U_G = 19.57$ m/s $U_L = 2.83$ m/s	$R_G = 0.091$ $R_L = -0.023$

The air deviation ratios R_G for point u, v and p are negative for distributor position 0° (horizontal) as shown in Table 3 and Fig. 5(a) with arrows sign. It means that for this condition, both air and water tend to flow out at lower outlet (see flow pattern image in Table 3), almost no fluid flow out at the upper outlet in this condition. When the superficial velocity both air and water are very low, most of the air accompanies with the water flowing out from the lower outlet.



(a) Superficial Velocity on Deviation Ratio.



(b) Mandhane [10] and Baker [11] Map for Horizontal Flow.

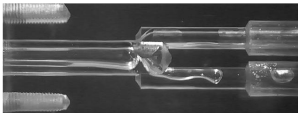
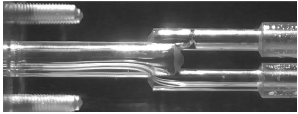
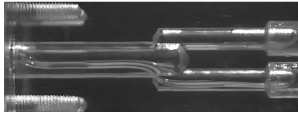
Fig. 5. Experimental Conditions in Circle Mark on Deviation Ratio and Flow Pattern Maps for 0°.

Figure 6 shows the experimental results of distributor position 45° (inclined) with deviation ratio on superficial velocities of air and water which are 0.06, 0.7, 17.92 m/s for air and 0.03, 0.33, 3.54 m/s for water, respectively. Figure 6(a) shows the superficial velocity for air and water with deviation ratio, where the experimental results marked with a circle.

Deviation ratio is positive for air (R_G) and negative for water (R_L). Figure 6(b) shows the flow pattern map of Mandhane [10] and Baker [11] at inclined position 45° with circle mark for experimental results. This circle is match with the circle in Fig 6(a). At water superficial velocity constant on 0.03, 0.33, 3.54 m/s with air superficial velocity is varied from 0.06 m/s to 17.92 m/s, the flow distribution of

air tends to even distribution at high air superficial velocity. Although the air deviation ratio R_G at point e is bigger than the point o and y , it is resulted of inclined position 45° and high air superficial velocity; air tends to flow out at upper outlet because of gravity.

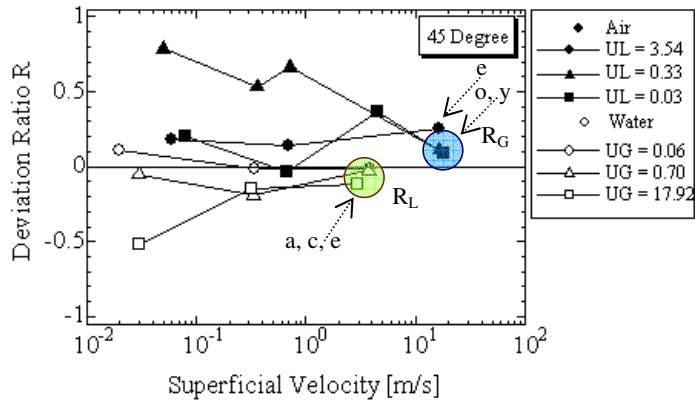
Table 3. Experimental Conditions for Point of u , v , and p at varies Superficial Velocities of Air and Water at Distributor position 0° (Horizontal).

Flow Pattern Image	Point	Superficial Velocity	Deviation Ratio
 Stratified flow	u	$U_G = 0.07$ m/s $U_L = 0.03$ m/s	$R_G = -0.464$ $R_L = -0.753$
 Stratified flow	v	$U_G = 0.16$ m/s $U_L = 0.03$ m/s	$R_G = -0.916$ $R_L = -1$
 Stratified flow	p	$U_G = 0.07$ m/s $U_L = 0.06$ m/s	$R_G = -0.462$ $R_L = -0.891$

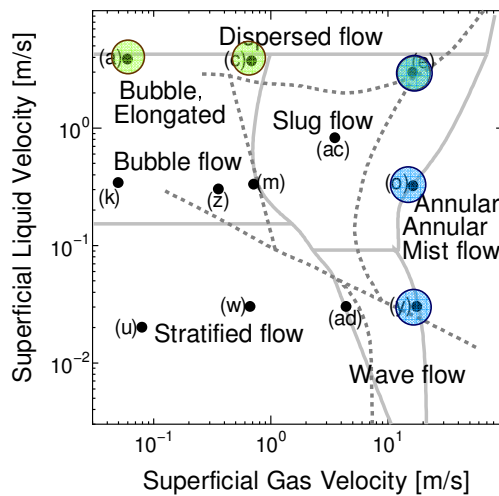
For all conditions, the air deviation ratios R_G are positive though they are rather close to zero, as shown in Fig. 6(a) with arrows (also see Tables 4 and 5). On the other hand, where the air superficial velocity is kept constant on 0.06, 0.7, 17.92 m/s and water superficial velocity is varied from 0.03 m/s to 3.54 m/s, the water deviation ratios R_L are negative though the values are approaching zero with increasing water superficial velocity. It means that the flow distribution of water tends to evenly distribution with increasing water superficial velocity. So it showed that equal flow distribution through the distributor at inclined position 45° occurs at high superficial velocities of air and water.

The flow pattern image for point y , o and e at distributor position 45° (inclined) are shown in Table 4, where the air superficial velocity is kept at high velocity around 17 m/s, and water superficial velocity is varied from 0.03 m/s to 2.97 m/s.

At this condition, equal distribution of air achieved with decreasing water superficial velocity. Compare to Table 2, it showed that the air flow distribution tends more uneven distribution than experimental condition in Table 2. On the other hand, the water deviation ratios R_L are negative, though the values are approaching zero and more evenly distribution achieved with increasing water superficial velocity. These are similar to experimental results in Table 2. The typical photographs of observed flow pattern as shown in Table 4, cover annular flow, annular mist flow and annular dispersed flow, it can be confirmed with Mandhane [10] and Baker [11] flow pattern map as shown in Fig. 6(b).



(a) Superficial Velocity on Deviation Ratio.



(b) Map [10, 11] for Horizontal Flow.

Fig. 6. Experimental Conditions in Circle Mark on Deviation Ratio and Flow Pattern Maps for 45°.

The flow pattern image for point *a*, *c* and *e* at distributor position 45° (inclined) are shown in Table 5 where the water superficial velocity is kept at high velocity around 3.54 m/s, and air superficial velocity is varied from 0.06 m/s to 16.37 m/s.

In this condition, the value of water deviation ratios R_L is approaching zero and evenly distribution achieved with increasing air superficial velocity. On the other hand, at water superficial velocity around 3.54 m/s, the air deviation ratios R_G are approaching zero with little discrepancy at point *e*, air tends to flow out at upper outlet because of gravity. The visualized flow regime as shown in Table 5 cover dispersed bubbly flow and annular dispersed flow; it can give good agreement with Mandhane [10] and Baker [11] flow pattern map as shown in Fig. 6(b).

Table 4. Experimental Conditions for Point of y , o , and e at varying Superficial Velocities of Water from Low to High and Air relatively Constant at Distributor Position 45° .

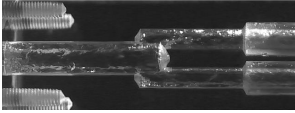
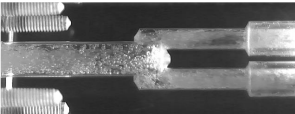
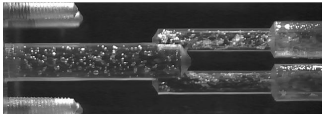
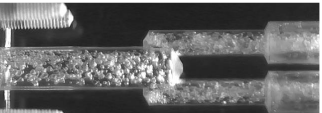
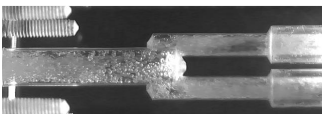
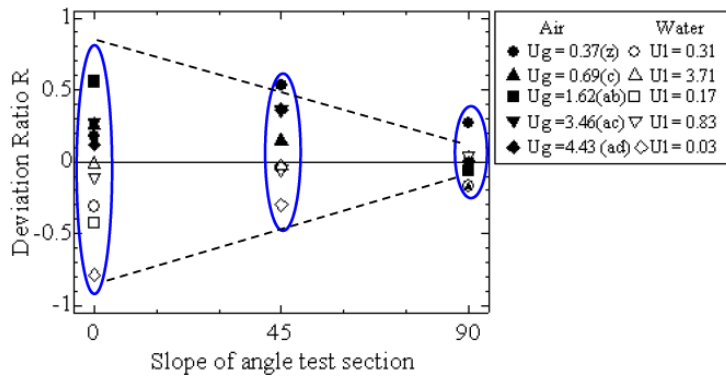
Flow Pattern Image	Point	Superficial Velocity	Deviation Ratio
 Annular flow	y	$U_G = 17.76$ m/s $U_L = 0.03$ m/s	$R_G = 0.097$ $R_L = -0.519$
 Annular mist flow	o	$U_G = 16.52$ m/s $U_L = 0.32$ m/s	$R_G = 0.112$ $R_L = -0.144$
 Annular dispersed flow	e	$U_G = 16.37$ m/s $U_L = 2.97$ m/s	$R_G = 0.251$ $R_L = -0.117$

Table 5. Experimental Conditions for Point of a , c , and e at varying Superficial Velocities of Air from Low to High and Water relatively Constant at Distributor Position 45° .

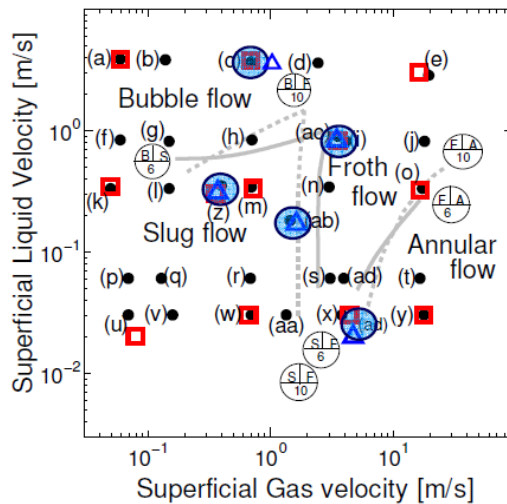
Flow Pattern Image	Point	Superficial Velocity	Deviation Ratio
 Dispersed bubbly flow	a	$U_G = 0.06$ m/s $U_L = 3.84$ m/s	$R_G = 0.178$ $R_L = -0.016$
 Dispersed bubbly flow	c	$U_G = 0.84$ m/s $U_L = 3.72$ m/s	$R_G = -0.042$ $R_L = 0.014$
 Annular dispersed flow	e	$U_G = 16.37$ m/s $U_L = 2.97$ m/s	$R_G = 0.251$ $R_L = -0.117$

Experimental results of distributor position in different inclination (angle 0° , 45° and 90°) on superficial velocities of air and water at point z , c , ab , ac , and ad are shown in Fig. 7(a). The flow pattern map of Mandhane [10] and Baker [11] in Fig. 7(b) shows the experimental conditions in which they are indicated the points with circle mark. In these conditions, the distribution of two-phase flow through

distributor tends unevenly flow distribution on horizontal position and tends evenly flow distribution on the vertical position as shown in Fig. 7(a) and Table 6. The deviation ratios R are approaching zero both for air and water with changing inclination from horizontal (0°) to vertical (90°). It can be concluded that the equal fluid distribution both air and water, it is achieved by changing the inclination angle from horizontal position to vertical position.



(a) Distributor Inclination on Deviation Ratio.

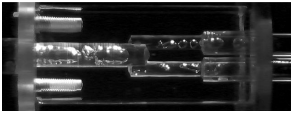
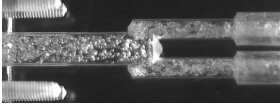
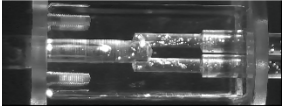
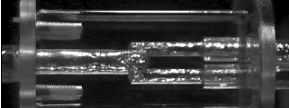
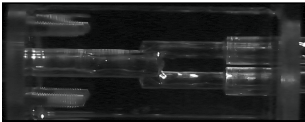


(b) Sekoguchi Map [12] for Vertical Flow.

Fig. 7. Experimental Conditions in Circle Mark on Deviation Ratio and Flow Pattern Maps for Different Inclination.

The observed flow pattern at point z , c , ab , ac , and ad at distributor position 90° (vertical) shown in Table 6 and it was plotted on Mandhane Baker map [10, 11] and Sekoguchi map [12] with circle mark for test results. The experimental results cover slug flow with small bubble, dispersed bubble flow, froth flow and annular flow. It can be confirmed with Sekoguchi flow pattern map [12] for vertical pipe with good agreement as shown in Fig. 4(b).

Table 6. Observed Flow Pattern for Point of z , c , ab , ac , and ad at Distributor Position 90° .

Flow Pattern Image	Point	Superficial Velocity	Deviation Ratio
 Slug flow	z	$U_G = 0.37$ m/s $U_L = 0.31$ m/s	$R_G = 0.268$ $R_L = -0.169$
 Dispersed bubble flow	c	$U_G = 0.95$ m/s $U_L = 3.7$ m/s	$R_G = -0.173$ $R_L = 0.029$
 Slug flow with small bubble	ab	$U_G = 1.62$ m/s $U_L = 0.17$ m/s	$R_G = -0.062$ $R_L = 0.029$
 Froth flow	ac	$U_G = 3.46$ m/s $U_L = 0.83$ m/s	$R_G = -0.029$ $R_L = 0.04$
 Annular flow	ad	$U_G = 4.71$ m/s $U_L = 0.02$ m/s	$R_G = -0.002$ $R_L = -0.077$

4. Conclusions

The experimental study was carried out to characterize the flow configurations and to clarify the distribution characteristics of air and water two-phase flow through the distributor. The observed flow pattern and the distribution deviation of two-phase flow were explained and the conclusions of this study could be drawn as follow:

- At the inlet of the distributor, the observed flow patterns of horizontal and vertical two-phase flows agreed well with the Mandhane-Baker flow map for horizontal flow and the Sekoguchi map for vertical flow, respectively.
- For horizontal and inclined conditions, the even distribution of two-phase flow in a distributor achieved only at high superficial velocities of both air and water.
- The deviation ratios R are approaching zero (even distribution) with increasing air and water superficial velocities and by changing the inclination angle from horizontal to vertical position. However, there is some inexplicable behavior and criteria of the even distribution have not been fully clarified.

References

1. Lee, J.K.; and Lee, S.Y. (2004). Distribution of two-phase annular flow at header-channel junctions. *Experimental Thermal and Fluid Science*, 28(2-3), 217-222.
2. Vist, S.; and Pettersen, J. (2004). Two-phase flow distribution in compact heat exchanger manifolds. *Experimental Thermal and Fluid Science*, 28(2-3), 209-215.
3. Marchitto, A.; Devia, F.; Fossa, M.; Guglielmini, G.; and Schenone, C. (2008). Experiments on two-phase flow distribution inside parallel channels of compact heat exchangers. *International Journal of Multiphase Flow*, 34(2), 128-144.
4. Yoshioka, S.; Kim, H.; and Kasai, K. (2008). Performance evaluation and optimization of a refrigerant distributor for air conditioner. *Journal of Thermal Science and Technology*, 3(1), 68-77.
5. Tae, S.J.; and Cho, K. (2003). Two-phase flow distribution and Phase separation through both horizontal and vertical branches. *KSME International Journal*, 17(8), 1211-1218.
6. Wen, M.Y.; Lee, C.H.; and Tasi, J.C. (2008). Improving two-phase refrigerant distribution in the manifold of the refrigeration system. *Applied Thermal Engineering*, 28(17-18), 2126-2135.
7. Kim, N.-H.; and Sin, T.-R. (2006). Two-phase flow distribution of air-water annular flow in a parallel flow heat exchanger. *International Journal of Multiphase Flow*, 32(12), 1340-1353.
8. Bell, Stephanie. (2001). *A Beginner's guide to uncertainty of measurement* (Issue 2). UK: National Physical Laboratory.
9. Moffat, R.J. (1988). Describing the uncertainties in experimental results. *Experimental Thermal and Fluid Science*, 1(1), 3-17.
10. Mandhane, J.M.; Gregory, G.A.; and Aziz, K. (1974). A flow pattern map for gas-liquid flow in horizontal pipes. *International Journal of Multiphase Flow*, 1(4), 537-553.
11. Baker, O. (1954). Design of pipelines for simultaneous flow of oil and gas. *Oil & Gas Journal*, 53, 185-195.
12. JSME. (2006). *Handbook of gas-liquid two-phase flow technology* (2nd Ed.). Japan: Corona Publishing Co. Ltd. (in Japanese).
13. Massoud, M. (2005). *Engineering thermo fluids (Thermodynamics, Fluid Mechanics, and Heat Transfer)* (1st Ed.). Germany: Springer-Verlag Berlin Heidelberg.
14. Ghiaasiaan, S. M. (2008). *Two-phase flow, boiling and condensation (In Conventional and Miniature Systems)* (1st Ed.). UK: Cambridge University Press.